

1-596
NATIONAL ADVISORY COMMITTEE FOR AERONAUTICS

JPL LIBRARY

CALIFORNIA INSTITUTE OF TECHNOLOGY

WARTIME REPORT

ORIGINALLY ISSUED

April 1945 as

Memorandum Report L5D09a

FLIGHT TESTS OF THE SIKORSKY HNS-1 (ARMY YR-4B) HELICOPTER

II - HOVERING AND VERTICAL-FLIGHT PERFORMANCE WITH THE

ORIGINAL AND AN ALTERNATE SET OF MAIN-ROTOR BLADES,

INCLUDING A COMPARISON WITH HOVERING

PERFORMANCE THEORY

By F. B. Gustafson and Alfred Gessow

Langley Memorial Aeronautical Laboratory
Langley Field, Va.



WASHINGTON

NACA WARTIME REPORTS are reprints of papers originally issued to provide rapid distribution of advance research results to an authorized group requiring them for the war effort. They were previously held under a security status but are now unclassified. Some of these reports were not technically edited. All have been reproduced without change in order to expedite general distribution.

COPY FILE

MR No. L5D09a

NATIONAL ADVISORY COMMITTEE FOR AERONAUTICS

MEMORANDUM REPORT

for the

Bureau of Aeronautics, Navy Department

and the

Army Air Forces, Air Technical Service Command

FLIGHT TESTS OF THE SIKORSKY HNS-1 (ARMY YR-4B) HELICOPTER
II - HOVERING AND VERTICAL-FLIGHT PERFORMANCE WITH THE
ORIGINAL AND AN ALTERNATE SET OF MAIN-ROTOR BLADES,
INCLUDING A COMPARISON WITH HOVERING
PERFORMANCE THEORY

By F. B. Gustafson and Alfred Gessow

SUMMARY

The results of hovering and vertical-flight performance tests conducted on an HNS-1 (Army YR-4B) helicopter are presented. Hovering data were obtained in the ground-effect region and at altitude with the original set of main-rotor blades. An alternate set of blades, provided for the tests by the Army Air Forces, was then tested in the hovering condition at altitude to determine whether significant differences in performance could be obtained by use of blades of different aerodynamic design and surface condition. The increased performance resulting from the use of the alternate set of blades enabled the determination of rotor efficiency in vertical climb.

Comparison of the hovering data obtained at altitude for the alternate set of blades with the corresponding data for the original set indicates an increase of more than 300 pounds in thrust available for hovering.

Data taken over a range of rotor speeds with the original blades showed that, as predicted by theory and by full-scale tunnel tests, appreciable power can be

1-596

saved by use of lower tip speeds. A saving of 10 horsepower, which corresponds to an increase in thrust available of about 130 pounds, was obtained by reducing the rpm from 2260 ($C_T = 0.0037$) to 1910 ($C_T = 0.0052$).

Good agreement was shown between the hovering results at altitude and existing theoretical performance-prediction methods. Values of thrust as high as 82 percent of the thrust calculated for an ideal rotor (that is, a rotor with zero profile-drag loss and uniform induced velocity) have been measured.

The power data obtained in the ground-effect region indicate that the most noticeable increase of power required with altitude occurs at the smallest ground clearances and that the effect becomes less marked with increasing altitude until little power change is felt above 30 feet. Preliminary data obtained at approximately 25 feet altitude indicate that the variation of power with speed between hovering and 10 miles per hour is probably not more than 2 to 3 percent.

Comparison of rotor shaft power in vertical climbs (at rates up to 650 feet per minute) with shaft power required in hovering shows that the increase in power actually required for climb is approximately half the rate of change of potential energy of the aircraft, indicating a corresponding increase in lifting efficiency in climb. Conversely, a similar comparison for rates of descent up to 450 feet per minute shows that the decrease in shaft power required is roughly half the rate of change of potential energy, indicating a corresponding decrease in lifting efficiency.

INTRODUCTION

As part of a general program of helicopter research requested by the Bureau of Aeronautics and the Air Technical Service Command, flight tests are being conducted at the LMAL with a Sikorsky HNS-1 (Army YR-4B) helicopter. The data thus obtained are being used to check existing performance theory and wind-tunnel measurements on powered lifting rotors and are being published as a series of reports covering the performance of the helicopter in various flight conditions. Level-flight performance is covered in Part I of the series.

The present report, Part II, deals with the vertical-flight performance including hovering in the ground-effect region and at altitude, and climb and descent conditions.

965-7
Following tests with the original main-rotor blades, an alternate set was tested in the hovering condition at altitude to determine whether significant changes in performance could be obtained with a rotor of different aerodynamic design and surface condition. This set, which was supplied by the Army Air Forces, was chosen from a group of five different sets of rotors because both theoretical considerations and full-scale tunnel tests indicated that it would yield the best performance in the conditions under which the tests were conducted. The results of these tests are compared with the data obtained for the original HNS-1 rotor and both sets of data are reduced to a nondimensional form and compared with the predictions of reference 1. In addition, the improved performance of the alternate rotor enabled vertical climb tests to be made so that rotor efficiency could be established in this condition as well as in hovering and vertical descent.

SYMBOLS

| | |
|----------|--|
| W | gross weight of helicopter, pounds |
| Ω | angular velocity of main-rotor blades, radians per second |
| R | radius of main-rotor blades, measured from axis of rotation to tip of blades, feet |
| v_c | rate of climb, feet per minute |
| V | true airspeed of helicopter |
| C_T | thrust coefficient $\left(\frac{W}{\rho(\Omega R)^2 \pi R^2} \right)$ |
| C_P | power coefficient $\left(\frac{\text{main-rotor shaft power}/\Omega R}{\rho(\Omega R)^2 \pi R^2} \right)$ |

- C_{P_c} power coefficient measured in climb
- C_{P_o} power coefficient which would be required to hover at the thrust coefficient occurring at a given rate of climb
- $C_{P.P.E.}$ that part of the power coefficient in climb represented by the rate of change of potential energy of the helicopter equal to

$$\frac{W(v_c)}{\rho (\Omega R)^2 \pi R^2 (\Omega R)}$$

- σ solidity, $bc_e/\pi R$,

where c_e = equivalent chord $\pm \frac{\int_0^R cr^2 dr}{\int_0^R r^2 dr}$

and c = actual blade chord at a distance r from the axis of rotation

- a slope of lift coefficient against section angle of attack (radian measure), assumed equal to 5.75 in this report
- h altitude of helicopter referenced to a horizontal plane intersecting the main rotor at the blade $3/4$ radius, feet
- V_{h6} wind speed measured at altitude of 6 feet (h_6), miles per hour
- V_h wind speed at altitude as calculated from the relation
- $$V_h = V_{h6} \left(\frac{h}{h_6} \right)^{1/5}, \text{ miles per hour}$$
- ρ mass density of air, slugs per foot³
- ρ_o mass density of air at sea level under standard conditions (0.002378 slug per foot³)

The present report, Part II, deals with the vertical-flight performance including hovering in the ground-effect region and at altitude, and climb and descent conditions.

965-7
Following tests with the original main-rotor blades, an alternate set was tested in the hovering condition at altitude to determine whether significant changes in performance could be obtained with a rotor of different aerodynamic design and surface condition. This set, which was supplied by the Army Air Forces, was chosen from a group of five different sets of rotors because both theoretical considerations and full-scale tunnel tests indicated that it would yield the best performance in the conditions under which the tests were conducted. The results of these tests are compared with the data obtained for the original HNS-1 rotor and both sets of data are reduced to a nondimensional form and compared with the predictions of reference 1. In addition, the improved performance of the alternate rotor enabled vertical climb tests to be made so that rotor efficiency could be established in this condition as well as in hovering and vertical descent.

SYMBOLS

| | |
|----------|--|
| W | gross weight of helicopter, pounds |
| Ω | angular velocity of main-rotor blades, radians per second |
| R | radius of main-rotor blades, measured from axis of rotation to tip of blades, feet |
| v_c | rate of climb, feet per minute |
| V | true airspeed of helicopter |
| C_T | thrust coefficient $\left(\frac{W}{\rho(\Omega R)^2 \pi R^2} \right)$ |
| C_P | power coefficient $\left(\frac{\text{main-rotor shaft power}/\Omega R}{\rho(\Omega R)^2 \pi R^2} \right)$ |

- C_{p_c} power coefficient measured in climb
- C_{p_o} power coefficient which would be required to hover at the thrust coefficient occurring at a given rate of climb
- $C_{p.P.E.}$ that part of the power coefficient in climb represented by the rate of change of potential energy of the helicopter equal to

$$\frac{W(v_c)}{\rho (\Omega R)^2 \pi R^2 (\Omega R)}$$

- σ solidity, $bc_e/\pi R$,
 where c_e = equivalent chord $= \frac{\int_0^R cr^2 dr}{\int_0^R r^2 dr}$
 and c = actual blade chord at a distance r from the axis of rotation

- a slope of lift coefficient against section angle of attack (radian measure), assumed equal to 5.75 in this report
- h altitude of helicopter referenced to a horizontal plane intersecting the main rotor at the blade $3/4$ radius, feet
- V_{h6} wind speed measured at altitude of 6 feet (h_6), miles per hour
- V_h wind speed at altitude as calculated from the relation

$$V_h = V_{h6} \left(\frac{h}{h_6} \right)^{1/5}, \text{ miles per hour}$$

- ρ mass density of air, slugs per foot³
- ρ_o mass density of air at sea level under standard conditions (0.002378 slug per foot³)

APPARATUS

969-7
Description of aircraft.- The dimensions and other details of the HNS-1 helicopter are given in Part I (reference 2). The plan form of the original and alternate main-rotor blades are shown in figure 1. In connection with the present series of tests, the following additional information is given:

Height of plane of main-rotor flapping hinges above ground (tires undeflected and shock struts extended), ft 9.0

| | Original (HNS-1 production) | Alternate (twisted plywood) |
|---|-----------------------------------|-----------------------------------|
| Main rotor characteristics: | | |
| Radius, ft | 19 | 19 |
| Blade twist, deg (linear) . . | None | -8.5 |
| Solidity, $bc_e/\pi R$ | 0.060 | 0.042 |
| Blade area (total, three blades), sq ft | 65.4 | 46.3 |
| Blade section | NACA 0012 | NACA 23015 (mod.) |
| Moment of inertia of blade about flapping axis, lb-ft-sec ² . | 146 | 163 |
| Blade weight (one blade), lb | 53 | 59 |

The original HNS-1 main-rotor blades used in the flight tests were the production model YR-4B fabric-covered blades as described in reference 3. The forward 35 percent of the chord was contoured by spruce fairing strips and the trailing edge was formed by wire cable. The fabric surface was not aerodynamically smooth because of the waves formed by the failure of the dope finish to entirely fill the hollows formed by the fabric weave. Also, the comparatively widely spaced ribs which formed the blade contour permitted surface distortion under load. (See reference 4.) The blades were wiped clean before each flight, but no attempt was made to alter the contour or to improve the original surface condition. When necessary, however, the blade leading edge was touched up with dope to offset the effects of abrasion.

The alternate set of main-rotor blades were plywood-covered and were constructed with an 8° twist, the pitch decreasing linearly from root to tip. A brass abrasion strip extended for a length of 100 inches inboard from the tip. The blades were waxed prior to the first flight. Much of the blade surface was aerodynamically smooth, but at the extreme leading edge and various local areas pitting or grain was noticed. Inspection of the blade contour revealed flat spots and other lack of fairness at numerous points. Also, between the leading-edge strip and the plywood covering, there was a U-shape furrow approximately $1/64$ to $1/32$ inch wide and deep. In spite of the application of filler to the most pronounced discontinuities the contour of the blades as tested did not represent a true airfoil section. Chordwise slits caused by small trim tabs located at the outboard end of the blades near their trailing edges were sealed with scotch tape before flight.

Instrumentation and methods.- Part or all of the following quantities were measured during the hovering, climb, and descent tests:

- Airspeed
- Rotor rpm
- Engine manifold pressure
- Main-rotor shaft torque
- Tail-rotor shaft torque
- Free-air temperature
- Intake-air temperature
- Free-air static pressure
- Main-rotor pitch
- Tail-rotor pitch

The methods by which the above quantities were obtained are fully described in reference 2. A special procedure, however, was adopted to measure altitude and airspeed during the ground-effect tests. The altitude of the helicopter was obtained by means of 35-millimeter movie-camera observations of the difference in height of the craft while on the ground and in the air. Its ground speed was determined from a calibration of camera speed together with camera records showing the position of the helicopter referenced to fixed ground objects. Wind speed and direction at a height of 6 feet were periodically measured throughout the flight at two anemometer stations placed several hundred feet on either side of the flight path. The airspeed of the helicopter was

then obtained by a vector addition of ground and wind speeds. Yaw angles were calculated as the difference between the air-flow direction as given by this vector addition and the helicopter flight-path direction.

RESULTS

Ground-effect data.- A summary of the data obtained with the original HNS-1 main-rotor blades in the ground-effect region is presented in table I. The effect of rpm on the power required for sustentation at various altitudes in the ground-effect region is shown in figure 2. A hovering point obtained at approximately 400 feet altitude and a point representing an average of data obtained in the ground-effect region in a later flight are included for comparison. The wind speeds shown on the figure start at the average measured value of 5.5 miles per hour (determined at 6 feet) and vary as the $1/5$ power of the altitude. This assumed variation of wind speed with altitude is an average of values suggested by several sources and is very similar to data presented in reference 5 as typical of velocity gradients above airports. The airspeeds given in table I were also obtained by use of this assumed gradient. Figure 3 indicates the effect of speed on power required at low altitudes in the near hovering condition.

In figures 2 and 3, the altitude of the helicopter is referenced to a horizontal plane in the rotor, intersecting the blades at their $3/4$ radius. The coning angles used in determining the reference plane were calculated by means of equations listed in reference 6.

Hovering at altitude.- Hovering data obtained at altitude with each set of main-rotor blades are presented in table II and are shown in terms of thrust and torque coefficients in figures 4 and 5. In the calculation of thrust coefficients, no allowance was made for the download on the fuselage; an estimate of the magnitude of this download indicated that it was of the order of 1 percent. Hovering data for the original rotor at 25 feet altitude, obtained from the faired curves of figure 2(a), are also shown in figure 4. The hovering performance of the two sets of rotors is then compared in figure 6.

Theoretical performance curves, as computed from Technical Note No. 626 (reference 1) for constant-chord blades, are plotted on the figures for purposes of comparison. The curve of ideal rotor performance, as represented by uniform induced velocity and zero profile-drag loss, was calculated on the basis of an ideal figure of merit equal to unity, that is,

$$M = 0.707 \frac{C_T^{3/2}}{C_Q} = 1$$

The performance curves for the nontwisted or "constant-incidence" blades are based on the semiempirical performance-prediction curves of figure 15 of reference 1. The performance of the ideally twisted or "constant pitch" rotor blade has been computed from the theoretical relations given by equations 13 and 16 in reference 1. The profile-drag terms used in equation 16 are based on the same profile-drag curve as that used for the constant-incidence case. The equation of this curve is

$$c_{d_0} = 0.01 + 0.3a^2$$

where a is the section angle of attack, referenced to the zero lift line and expressed in radians. At the thrust coefficients covered in these tests the use of this drag curve is approximately equivalent to the use of a mean drag coefficient of 0.012 in the calculations for solidity 0.06 (original blades) and 0.014 for solidity 0.042 (alternate blades).

Vertical climbs and descents.— Data obtained in vertical descent are listed in table II, and data obtained from continuous records in vertical climb are plotted in figure 7. The climb and descent data for the alternate rotor blades, plotted in coefficient form, are given in figure 8. The power coefficient C_{P_0} was calculated from the power required to hover at the thrust coefficient at which the rate of climb occurred. This hovering power was obtained from the measured values plotted in figure 5. The coefficient $C_{P.E.}$ represents the power corresponding to the rate of change of potential energy of the aircraft in the climb or descent condition, calculated

from the known gross weight and the measured rates of climb as follows:

$$C_{PP.E.} = \frac{W(v_c)}{\rho(\Omega R)^2 \pi R^2(\Omega R)}$$

Thus the curve labeled $\frac{C_{P_o} + C_{PP.E.}}{C_{P_o}}$ represents the

climb power required at various rates of climb that would be expected if there were no change in the induced or profile power losses due to the climb velocity, while the curve C_{P_c}/C_{P_o} indicates the actual climb power required.

DISCUSSION

Ground-effect data.- The effect of rpm on the power required for sustentation is clearly indicated by figure 2. A reduction in power required of approximately 9 horsepower in main-rotor power (fig. 2(a)) and 10 to 11 horsepower in total shaft power (fig. 2(b)) is shown for operation at 1910 rpm. Over the range of heights covered, the magnitude of the saving does not appear to be influenced by the amount of ground effect present. Theory and tunnel tests on full-scale rotors (reference 3) show these same trends over a wider rpm range.

It is evident that greater take-off thrusts would be obtained if the engine-rotor gear ratio were changed to permit operation at lower tip speeds while still drawing rated engine power. Theoretical considerations indicate, however, that if such low tip speeds were used in forward flight, tip stall and the associated instability and loss of power would result when operating at or near top speed; this view is confirmed by the pilot's observations that the aircraft became uncontrollable at rpm's below 1900 in level flight at full throttle and that control was already difficult at 1900 rpm. (See "Discussion," Part I.) Since the present top speed for 1900 rpm is quite low, the indication is that, if optimum or near-optimum hovering performance is desired without sacrifice in top speed, a gearshift will be necessary.

Theoretical treatments of ground effect in hovering in still air (reference 7) indicate changes in power required with altitude similar in character to those shown on figure 2. Although the presence of an indeterminate wind gradient in the tests preclude detailed comparison with theory, it is evident that under practical conditions the rotor height does have a critical effect on the power required to lift the aircraft from the ground and that most of this effect has been lost when an altitude of approximately 30 feet has been reached.

Figure 3 was included to provide some basis for estimating the effect of the outer limits of speed present during the measurements of figure 2. It indicates that approximately half of the power difference shown in figures 2(a) and 2(b) at 50 feet altitude as compared with 400 feet altitude is accounted for by the difference in the airspeed present in the tests at the two altitudes. The data of figure 3, which were obtained at heights of approximately 20 and 30 feet, also involve the estimation of the wind gradient; the average measured wind velocity at 6 feet was 6 miles per hour. Because the data do not extend quite to zero airspeed and because of the scatter shown by the test points, they should be viewed as preliminary. This figure is nevertheless felt to afford the best available indication of the effect of low airspeeds on power required under the conditions represented.

Hovering at altitude.— Inspection of figure 4 indicates that, at normal take-off power and rpm (full throttle, 2250 rpm, $C_Q^{2/3} \approx 0.0043$), the original blades will produce 72 percent of the thrust that would be generated by an ideal rotor (that is, one with zero profile-drag loss and with uniform induced velocity). The figure also shows that available performance theory for blades of constant chord and blade angle provides predictions in reasonable agreement with the experimental data. A comparison of the drag curve used in the theoretical treatment with experimental data obtained by two-dimensional tunnel tests on a practical-construction Sikorsky YR-4A specimen (reference 4) subjected to various internal pressures indicated that the actual profile-drag values for the original blade were probably somewhat higher than those assumed, but measurements of blade internal pressure in flight are needed before detailed conclusions can be drawn in this regard.

1-596

In a similar manner, the data shown in figure 5 reveals that the alternate rotor yielded 82 percent of the thrust produced by an ideal rotor and that reasonable agreement with theory is obtained. However, inasmuch as no wind-tunnel profile-drag data are available for practical-construction blade specimens of construction corresponding to that of the alternate blades, no detailed or precise comparison with theory can be made.

The curves for ideal blade twist (twist theoretically needed for uniform induced velocity) shown in figures 4 and 5 may be used to estimate the possible magnitude of the effects of the taper and twist present in the blades tested. The gap between these curves and the curves representing constant blade-angle performance represents the maximum savings in induced power that could be obtained by twist or taper.

The comparison of performance of the original and the alternate set of rotor blades afforded by figure 6 shows that, at normal take-off rpm and full throttle (2250 rpm, $C_Q^{2/3} \approx 0.0043$), the alternate rotor could produce 330 pounds more thrust than the original rotor. In attempting to judge the source of this difference in performance, the effects of the following factors must be weighed: (a) solidity; (b) twist; (c) plan form; (d) airfoil section, including both thickness and camber; (e) blade surface roughness, accuracy of contour, and surface deformation in flight; and (f) Reynolds number.

It is not possible to evaluate the individual effects of each of these variables on rotor performance from test data now available. However, it is believed that items (a), (b), and (e) are most important in the present case and that the following qualitative statements would be helpful in interpreting the test results:

(a) A study of figures 4 and 5 reveals that approximately one-half of the performance difference may be accounted for by the lower solidity of the alternate rotor. Although combinations of high solidities and low tip speeds are, in general, expected to be most efficient in the hovering condition, a reduction in solidity is advantageous when the tip speed is fixed and the blade sections are operating at an angle of attack below the optimum. Thus in the present case, the 0.042 solidity rotor operated at mean blade angles of

attack closer to the optimum than did the 0.060 solidity rotor with a consequent saving in profile-drag power.

(b) The alternate rotor would be expected to operate at a lower induced loss than the original rotor because of the incorporation of some twist in the alternate set of blades. Examination of the problem suggests, however, that in this connection other combinations of twist and plan form might be made to produce still better results.

(e) The blade surface condition affects the total rotor losses to a significant degree. This fact has been shown theoretically in figure 3 of reference 8, and demonstrated experimentally in reference 3. The plywood-covered set of rotor blades would therefore be expected to require less power because of their smoother and more rigid surface.

These considerations indicate that still better hovering performance can be achieved through further refinement in aerodynamic design and further improvement in surface condition. In connection with refinement of aerodynamic design it is believed that an extension of the theory of NACA Technical Note No. 626 (reference 1) to include the effects on hovering performance of various combinations of taper and twist would be desirable.

Vertical climbs and descents.- Vertical velocities are expected to result in pronounced changes in the power required to produce lift as contrasted with that required for the same purpose in hovering. An inspection of figure 8 reveals that over the range of climb velocities covered (from 0 to 650 feet per minute) a saving in power equal to 45 percent of the power corresponding to the rate of change of potential energy of the helicopter is realized because of changes in induced and profile power. From the small amount of data obtained in the descent condition, it appears that the percentage of the potential energy power that is not recovered varies from approximately 70 percent at small rates of descent (<200 feet per minute) to approximately 50 percent at 450 feet per minute. These power changes obtained in the climb and descent conditions are approximately equal to the changes in induced power loss predicted by simple momentum theory.

Figure 8 also indicates that interpolation of the climb and descent data predicts measured hovering power within the neighborhood of 1 percent. Thus, the extrapolation of vertical-descent data to zero descent velocity appears to offer promise as a method of predicting the power required to hover for an overloaded helicopter or one operating in rarified atmosphere. A check on the power required for hovering at altitude with the original set of blades was secured by this procedure. Descent data listed in table II for the original rotor were obtained at a rate of descent of 142 feet per minute and were extrapolated to the hovering condition by means of figure 8. The estimated hovering point thus obtained, together with actual hovering points, are shown in figure 4. However, before detailed use is made of this method, it would be desirable to determine the shape of the C_{p_c}/C_{p_o} curve for blades of several different aerodynamic designs.

CONCLUSIONS

Flight tests have been conducted on the HNS-1 helicopter as equipped with two different sets of main-rotor blades. From the hovering and vertical-flight performance data obtained thus far, the following conclusions may be drawn.

1. An increase in thrust available for hovering at altitude of more than 300 pounds has been obtained by replacing the original set of main-rotor blades by one of different aerodynamic design and surface condition.
2. As predicted by theory and by full-scale tunnel tests, appreciable power was saved by use of low tip speeds. A saving of 10 horsepower, which corresponds to an increase of thrust available for hovering of about 130 pounds, was obtained by reducing the rpm from 2260 ($C_T = 0.0037$) to 1910 ($C_T = 0.0052$).
3. The theory presented in NACA Technical Note No. 626 may be used to predict actual helicopter hovering performance with reasonable accuracy if the blade-section profile-drag polar is approximately known.

4. Values of thrust as high as 82 percent of the thrust produced by an ideal rotor (that is, a rotor with zero profile-drag loss and uniform induced velocity) have been obtained.

5. Power data obtained in the ground-effect region indicate that the most noticeable increase of power required with altitude occurs at the smallest ground clearances and that the effect becomes less marked with increasing altitude until little power change is felt above 30 feet.

6. Preliminary data obtained at approximately 25 feet altitude indicate that the variation of power with speed between hovering and 10 miles per hour is probably not more than 2 to 3 percent.

7. Comparison of rotor shaft power in vertical climbs (at rates up to 650 feet per minute) with shaft power required in hovering shows that the increase in power actually required for climb is approximately half the rate of change of potential energy of the aircraft, indicating a corresponding increase in lifting efficiency in climb. Conversely, a similar comparison for rates of descent up to 450 feet per minute shows that the decrease in shaft power required is roughly half the rate of change of potential energy, indicating a corresponding decrease in lifting efficiency.

Langley Memorial Aeronautical Laboratory
National Advisory Committee for Aeronautics
Langley Field, Va.

REFERENCES

1. Knight, Montgomery, and Hefner, Ralph A.: Static Thrust Analysis of the Lifting Airscrew. NACA TN No. 626, 1937.
2. Gustafson, F. B.: Flight Tests of the Sikorsky HNS-1 (Army YR-4B) Helicopter. I - Experimental Data on Level-Flight Performance with Original Rotor Blades. TED No. NACA 1301. NACA MR No. L5C10, 1945.
3. Dingeldein, Richard C., and Schaefer, Raymond F.: Static Thrust Tests of Six Rotor-Blade Designs on a Helicopter in the Langley Full-Scale Tunnel. NACA ARR No. L5F25b, 1945.
4. Tetervin, Neal: Airfoil Section Data from Tests of 10 Practical-Construction Sections of Helicopter Rotor Blades Submitted by the Sikorsky Aircraft Division, United Aircraft Corporation. NACA MR, Sept. 6, 1944.
5. Bradfield, F. B., and Cohen, J.: Wind Tunnel Tests of Lift and Drag Measured in a Velocity Gradient. R. & M. No. 1489, British A.R.C., 1932.
6. Bailey, F. J., Jr.: A Simplified Theoretical Method of Determining the Characteristics of a Lifting Rotor in Forward Flight. NACA Rep. No. 716, 1941.
7. Knight, Montgomery, and Hefner, Ralph A.: Analysis of Ground Effect on the Lifting Airscrew. NACA TN No. 835, 1941.
8. Gustafson, F. B.: Effect on Helicopter Performance of Modifications in Profile Drag Characteristics of Rotor-Blade Airfoil Sections. NACA ACR No. 14H05, 1944.

4-596

TABLE I
SUMMARY OF HOVERING DATA IN GROUND-EFFECT REGION;
HNS-1 HELICOPTER WITH ORIGINAL BLADES

| Flight | Run | h_w (ft) (1) | h (ft) | V_{h6} (mph) | V (mph) | ρ/ρ_0 | W (lb) | Rotor rpm | Engine rpm | Atmos. press. (in. Hg) | F.A.T. (°F) (2) | Manifold pressure (in. Hg) | Chart hp | Main rotor shaft hp | Tail rotor shaft hp | θ_m (deg) (3) | θ_t (deg) (4) | C_T | C_Q |
|--------|-----|----------------------|-------------|-------------------|--------------|---------------|-------------|--------------|---------------|------------------------------|-----------------------|----------------------------------|-------------|------------------------------|------------------------------|----------------------------|----------------------------|--------|----------|
| 11 | 1 | 15.3 | 27.0 | 5.5 | 7.0 | 0.990 | 2260 | 231 | 2160 | 30.30 | 68 | 24.4 | 152 | 127 | 11.2 | 8.2 | 4.1 | 0.0040 | 0.000270 |
| | 2 | 19.0 | 30.7 | 5.0 | 7.0 | .986 | 2251 | 231 | 2160 | 30.30 | 70 | 25.2 | 158 | 130 | 11.0 | 8.5 | 4.8 | .0040 | .000278 |
| | 3 | .8 | 12.3 | 5.0 | 6.0 | .990 | 2254 | 241 | 2250 | 30.30 | 68 | ---- | ---- | 116 | 10.0 | 7.0 | 3.0 | .0037 | .000218 |
| | 4 | 1.1 | 12.7 | 5.5 | 6.5 | .990 | 2254 | 241 | 2250 | 30.30 | 67 | ---- | ---- | 115 | 10.9 | 7.0 | 3.2 | .0037 | .000216 |
| | 5 | 4.1 | 15.7 | 5.0 | 6.0 | .992 | 2254 | 239 | 2240 | 30.30 | 66 | ---- | ---- | 121 | 10.8 | 7.2 | 3.7 | .0037 | .000230 |
| | 6 | 6.6 | 18.1 | 5.5 | 7.0 | .992 | 2254 | 244 | 2280 | 30.30 | 66 | ---- | ---- | 126 | 11.0 | 7.4 | 4.0 | .0036 | .000227 |
| | 7 | 13.8 | 25.4 | 5.5 | 7.5 | .987 | 2254 | 242 | 2260 | 30.30 | 69 | 24.5 | 160 | 131 | 11.5 | 7.6 | 3.8 | .0037 | .000243 |
| | 8 | 27.6 | 39.1 | 6.0 | 8.5 | .978 | 2248 | 245 | 2290 | 30.30 | 74 | 24.5 | 160 | 133 | 11.9 | 8.0 | 4.1 | .0036 | .000240 |
| | 9 | 1.3 | 13.5 | 7.0 | 8.5 | .998 | 2302 | 204 | 1910 | 30.30 | 63 | ---- | ---- | 110 | 8.3 | 9.3 | 4.8 | .0052 | .000336 |
| | 10 | 2.3 | 14.5 | 6.5 | 8.0 | .998 | 2302 | 205 | 1920 | 30.30 | 63 | ---- | ---- | 111 | 9.7 | 9.4 | 5.7 | .0051 | .000334 |
| | 11 | 6.6 | 18.8 | 6.0 | 8.0 | .998 | 2302 | 204 | 1910 | 30.30 | 63 | ---- | ---- | 117 | 9.2 | 9.7 | 6.4 | .0052 | .000357 |
| | 12 | 7.6 | 19.8 | 6.0 | 7.5 | .998 | 2302 | 204 | 1910 | 30.30 | 63 | 25.7 | 145 | 118 | 9.2 | 9.7 | 5.9 | .0052 | .000360 |
| | 13 | 12.0 | 24.2 | 6.0 | 7.5 | .992 | 2299 | 204 | 1910 | 30.30 | 66 | 26.9 | 153 | 121 | 9.2 | 10.1 | 6.1 | .0052 | .000373 |
| | 14 | 18.2 | 30.4 | 5.5 | 7.5 | .979 | 2299 | 205 | 1920 | 30.30 | 73 | 27.7 | 159 | 124 | 9.5 | 10.1 | 6.1 | .0052 | .000378 |

¹Altitude of helicopter referenced to bottom of wheels, struts extended and tires undeflected.

²Free-air temperature.

³Average main-rotor-blade pitch, uncorrected for play in linkage and for mean blade twist.

⁴Average tail-rotor-blade pitch, uncorrected for play in linkage and for mean blade twist.

NATIONAL ADVISORY
COMMITTEE FOR AERONAUTICS

TABLE II
SUMMARY OF DATA OBTAINED IN HOVERING AT ALTITUDE
AND IN VERTICAL DESCENT; HNS-1 HELICOPTER

| Flight | Run | v_c (fpm) | W (lb) | V_{hor} (mph) (1) | Atmos. press. (in. Hg) | ρ/ρ_0 | Rotor rpm | Engine rpm | F.A.T. (°F) (2) | Manifold pressure (in. Hg) | Chart hp | Main rotor shaft hp | Tail rotor shaft hp | θ_M (deg) (3) | θ_t (deg) (4) | C_T | C_Q | $C_Q^{\frac{2}{3}}$ |
|-----------------------------|-----|----------------|-----------|---------------------------|------------------------------|---------------|--------------|---------------|-----------------------|----------------------------------|-------------|------------------------------|------------------------------|----------------------------|----------------------------|--------|----------|---------------------|
| Original main-rotor blades | | | | | | | | | | | | | | | | | | |
| 12 | 32 | 0 | 2280 | <5 | 29.75 | 0.972 | 228 | 2130 | 70 | 26.6 | 165 | 138 | 9.8 | 9.1 | 5.1 | 0.0042 | 0.000328 | 0.00475 |
| 19 | 3 | -142 | 2418 | 1. | 28.60 | .961 | 238 | 2220 | 55 | 27.7 | 179 | 146 | 11.5 | 8.9 | 5.0 | .0042 | .000294 | .00442 |
| Alternate main-rotor blades | | | | | | | | | | | | | | | | | | |
| 14 | 2 | 0 | 2369 | 4 | 29.65 | 1.026 | 222 | 2070 | 40 | 23.1 | 140 | 118 | ---- | 9.7 | 6.0 | 0.0044 | 0.000272 | 0.00420 |
| | 3 | 0 | 2363 | 5 | 29.65 | 1.026 | 225 | 2100 | 40 | 23.1 | 143 | 120 | ---- | 9.7 | 5.7 | .0043 | .000265 | .00413 |
| 15 | 2 | 0 | 2508 | 4 | 26.89 | .930 | 232 | 2160 | 40 | 26.1 | 166 | 138 | 10.0 | --- | 7.0 | .0047 | .000310 | .00458 |
| | 3 | 0 | 2506 | 4 | 26.87 | .930 | 230 | 2150 | 40 | 26.1 | 166 | 136 | 9.7 | --- | 6.9 | .0048 | .000311 | .00460 |
| | 4 | 0 | 2504 | 5 | 26.88 | .930 | 230 | 2170 | 40 | 26.1 | 166 | 139 | 9.5 | --- | 6.5 | .0047 | .000308 | .00456 |
| | 5 | 0 | 2502 | 4 | 26.96 | .931 | 232 | 2160 | 41 | 26.2 | 166 | 139 | 9.7 | --- | 6.8 | .0047 | .000311 | .00460 |
| | 6 | 0 | 2500 | 4 | 26.93 | .931 | 230 | 2150 | 40 | 26.2 | 166 | 137 | 11.0 | --- | 7.1 | .0047 | .000313 | .00461 |
| | 7 | 0 | 2490 | 4 | 27.01 | .934 | 230 | 2150 | 40 | 26.3 | 166 | 137 | 9.7 | --- | 6.9 | .0047 | .000312 | .00461 |
| | 8 | 0 | 2484 | 4 | 27.19 | .940 | 229 | 2140 | 40 | 26.4 | 164 | 135 | 10.4 | --- | 7.1 | .0047 | .000309 | .00456 |
| | 9 | 0 | 2478 | 0 | 26.97 | .925 | 229 | 2130 | 44 | 26.3 | 164 | 138 | 9.6 | --- | 7.1 | .0048 | .000324 | .00472 |
| | 10 | 0 | 2475 | 0 | 26.92 | .924 | 228 | 2130 | 44 | 26.2 | 164 | 137 | 9.6 | --- | 6.9 | .0048 | .000323 | .00471 |
| | 11 | -208 | 2469 | 3 | 27.35 | .941 | 229 | 2140 | 43 | 25.2 | 158 | 131 | 9.5 | --- | 6.2 | .0047 | .000300 | .00450 |
| | 12 | -154 | 2460 | 4. | 27.25 | .936 | 230 | 2140 | 43 | 25.0 | 157 | 130 | 9.9 | --- | 7.0 | .0047 | .000296 | .00445 |
| | 13 | -452 | 2448 | 4 | 27.44 | .943 | 227 | 2120 | 43 | 22.7 | 141 | 116 | 10.3 | --- | 7.0 | .0047 | .000271 | .00421 |

¹Horizontal component of air velocity.

²Free-air temperature.

³Average main-rotor-blade pitch, uncorrected for play in linkage and for mean blade twist.

⁴Average tail-rotor-blade pitch, uncorrected for play in linkage and for mean blade twist.

NATIONAL ADVISORY
COMMITTEE FOR AERONAUTICS

MR No. L5D09a

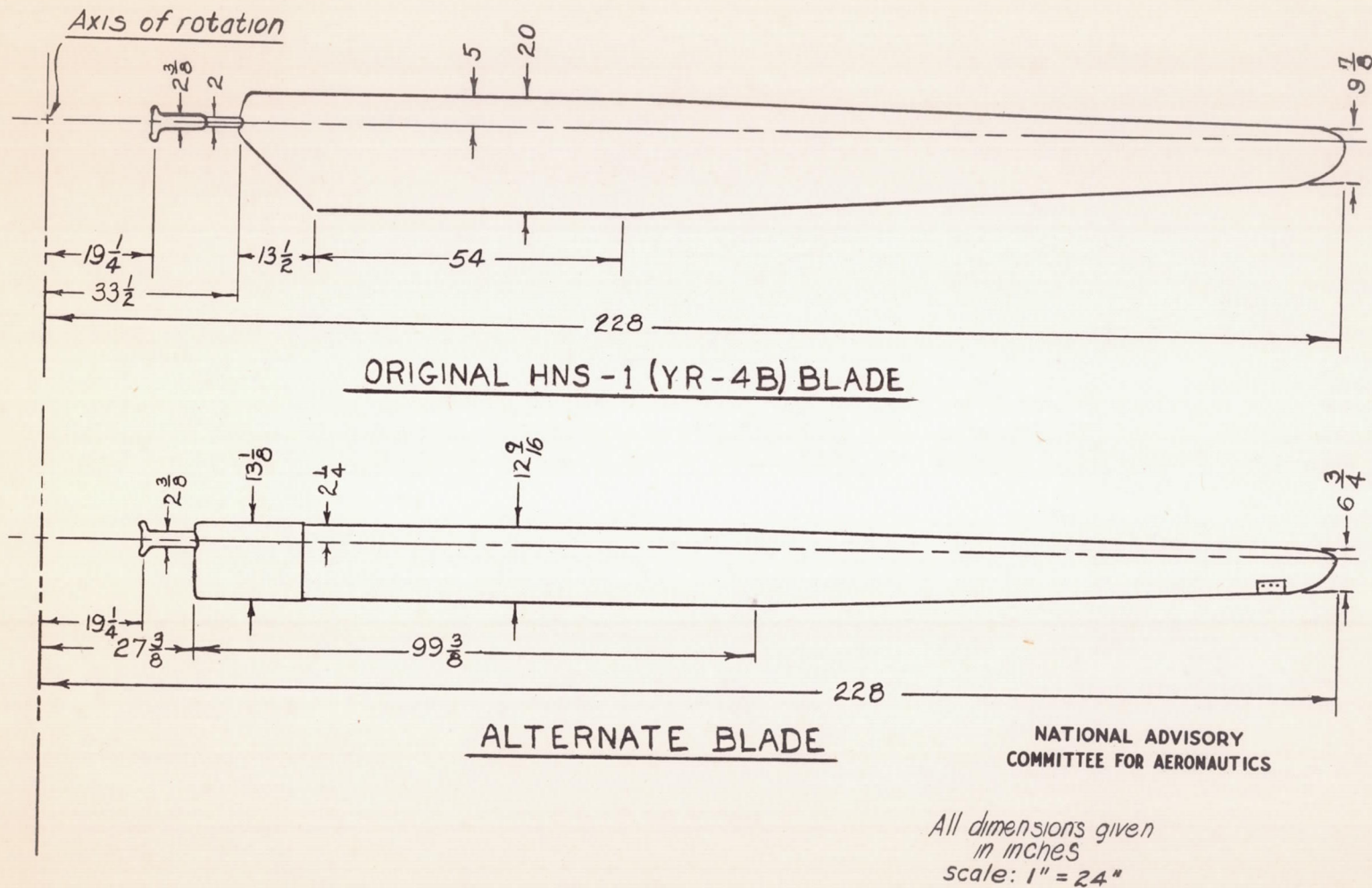


Figure 1.- Planform dimensions of original and alternate main-rotor blades; HNS-1 helicopter.

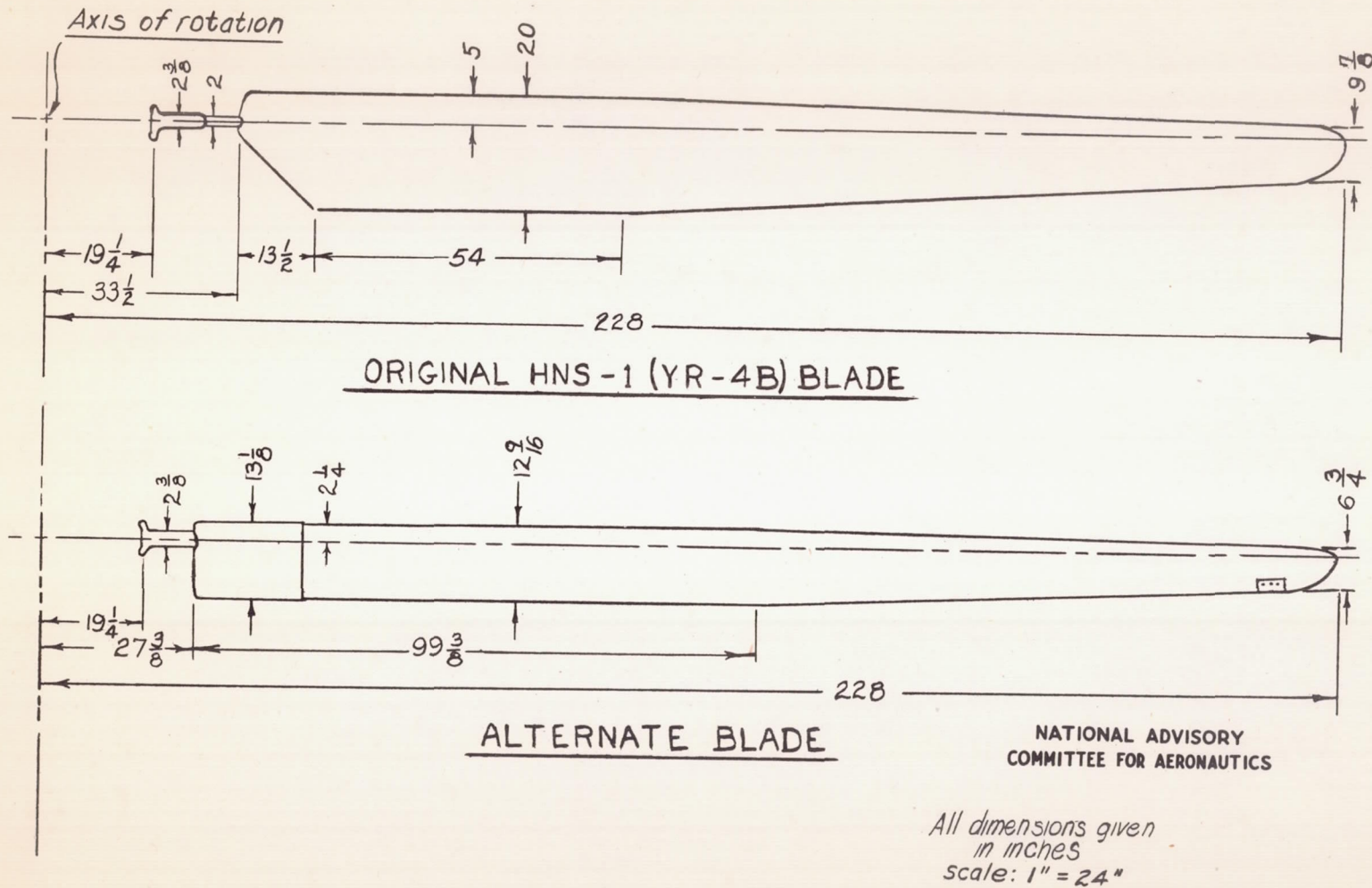
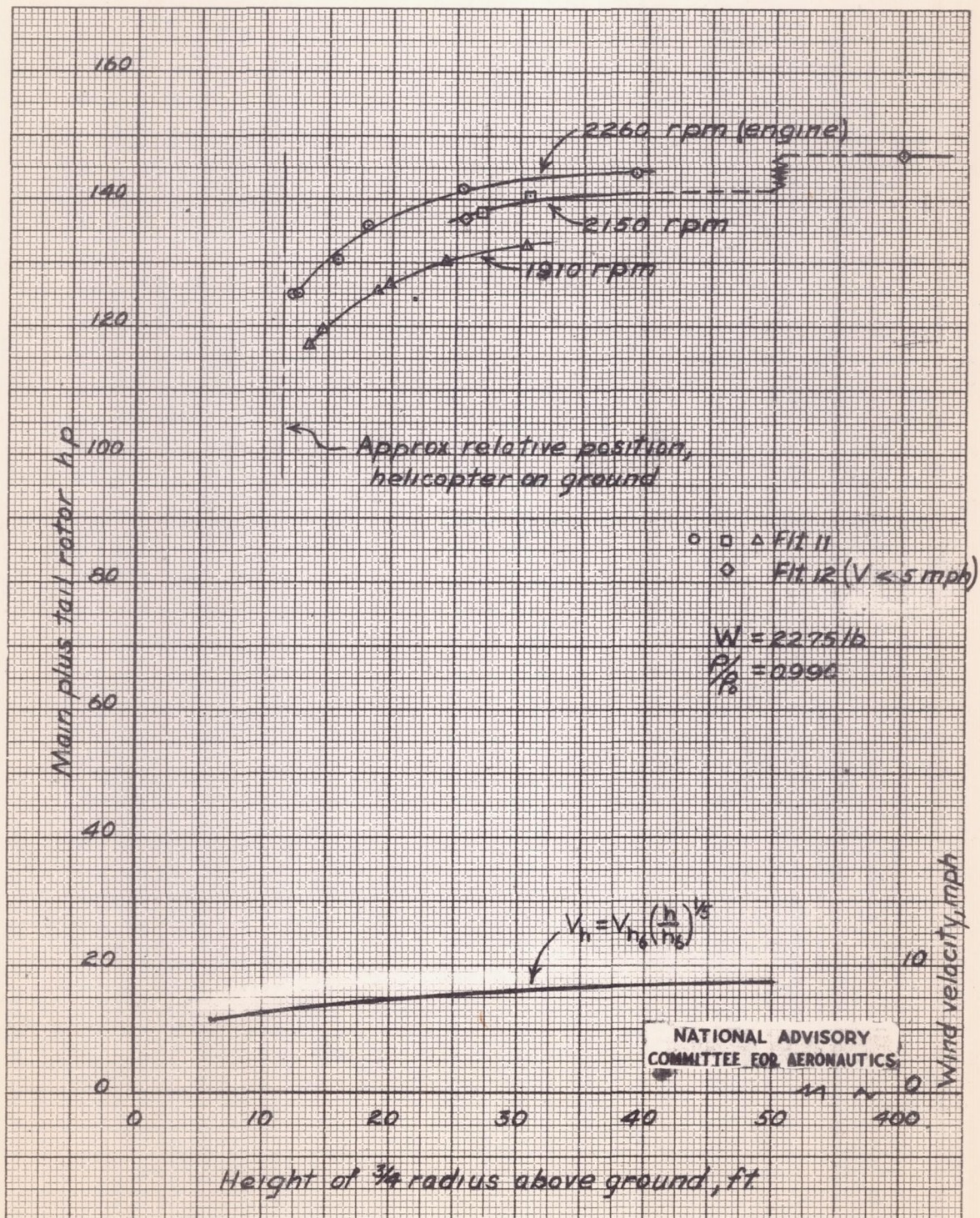


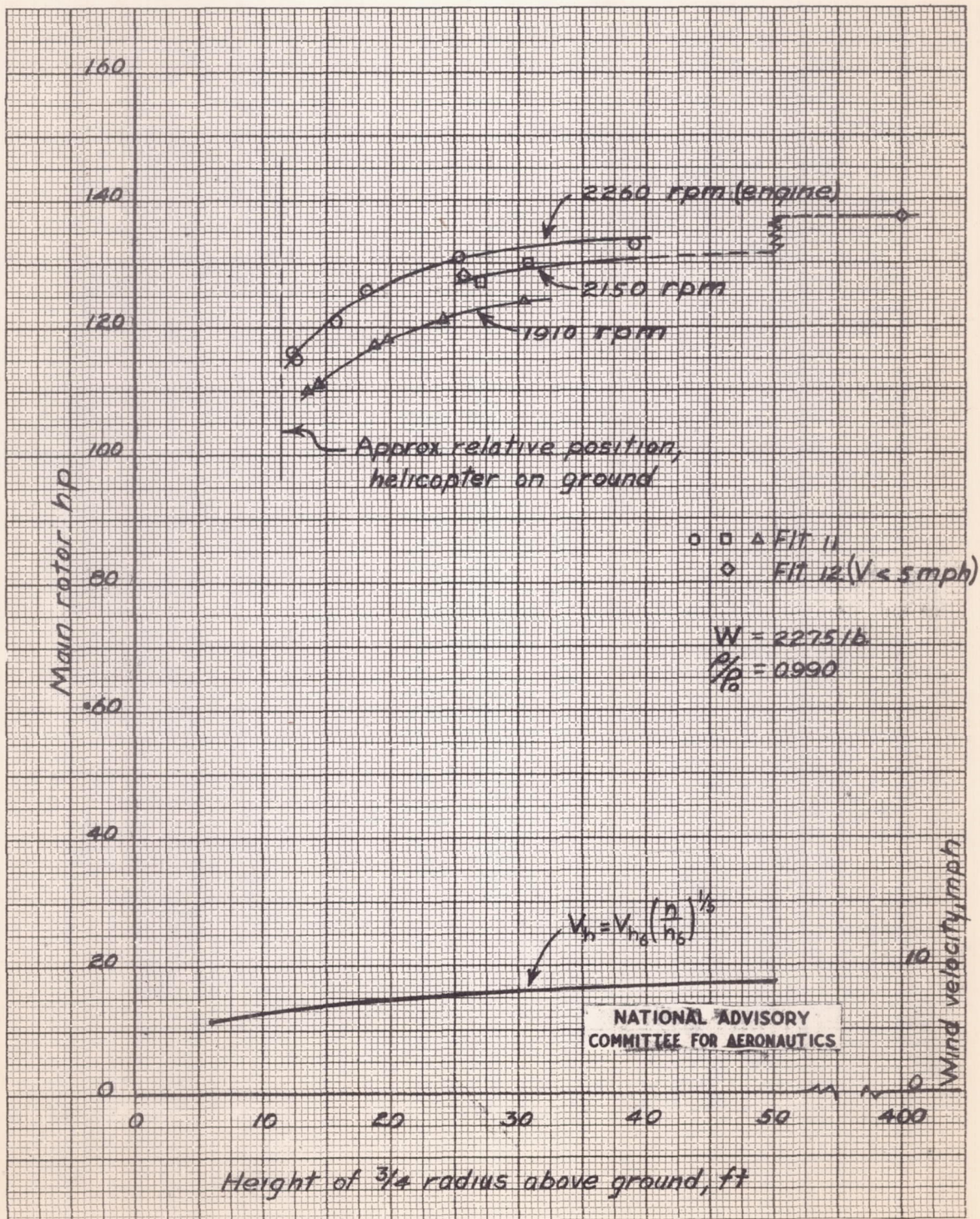
Figure 1.- Planform dimensions of original and alternate main-rotor blades; HNS-1 helicopter.

L-596



(b) Main plus tail rotor shaft power vs. height.

Figure 2.- Concluded.



(a) Main rotor shaft power vs. height

Figure 2.- Effect of rpm on the power required to hover in the ground effect region; HNS-1 helicopter with original main rotor blades.

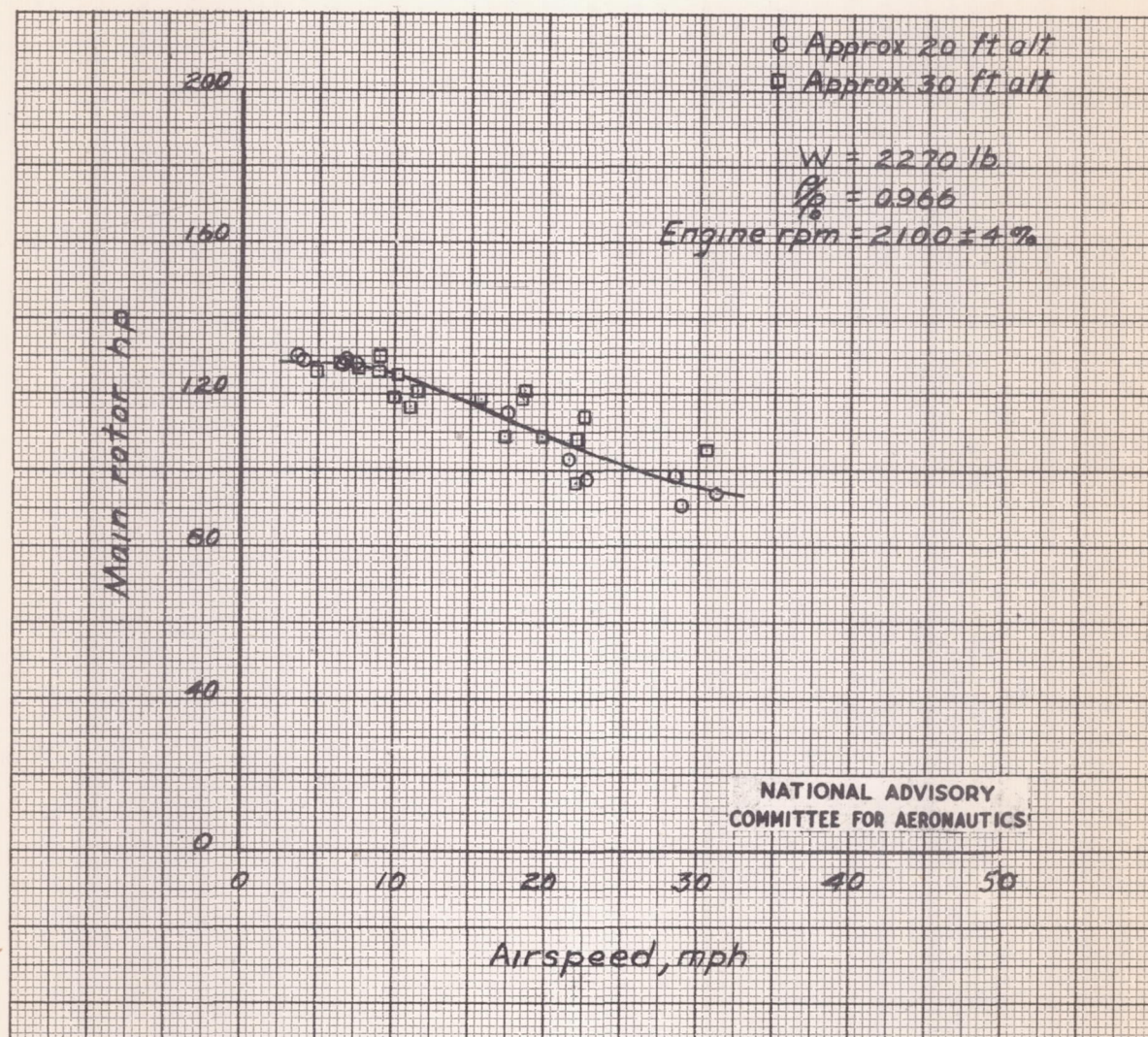


Figure 3.- Preliminary data indicating the effect of airspeed on the main rotor shaft power required by the HNS-1 helicopter in the near hovering condition.

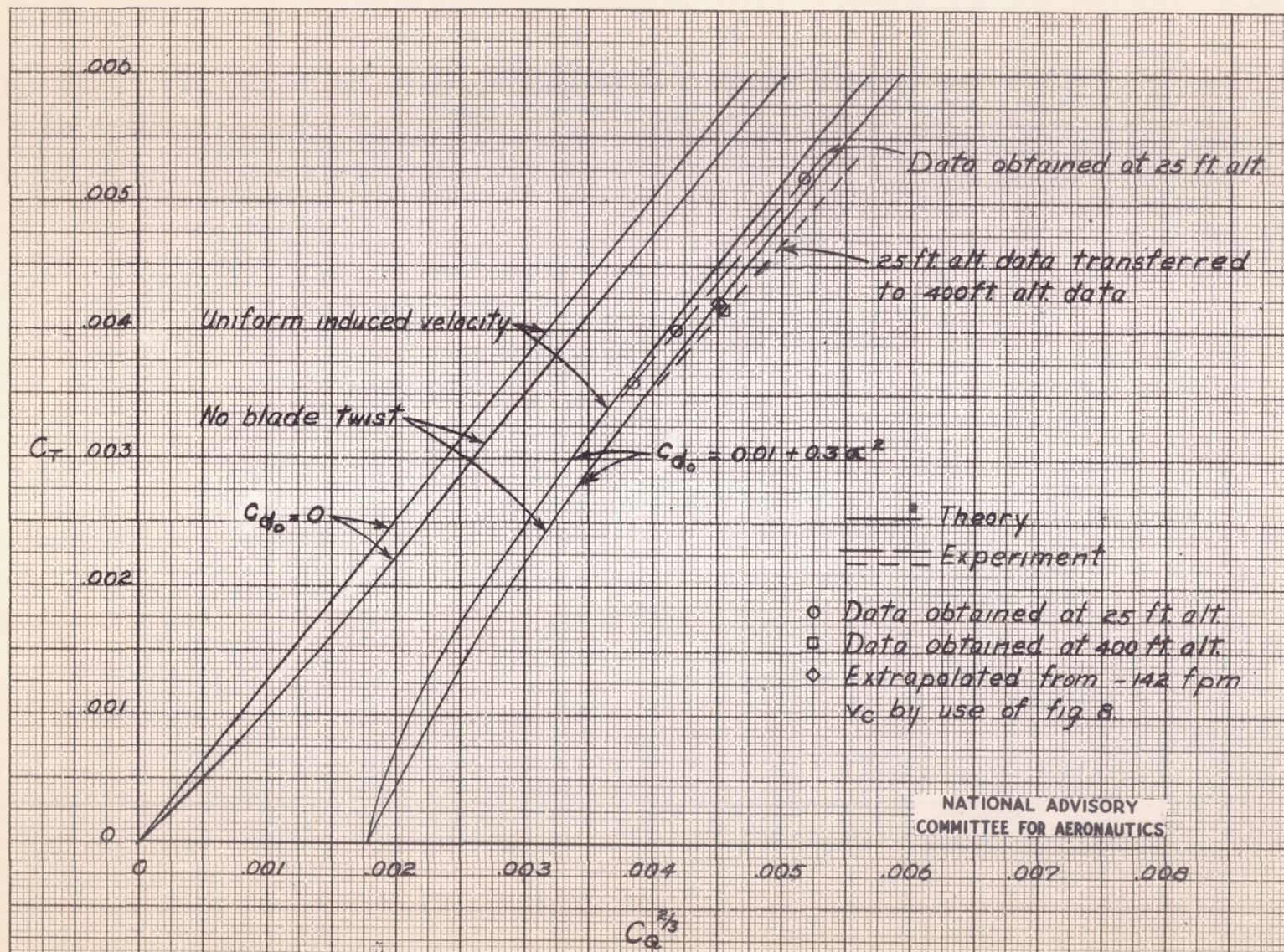


Figure 4.- Comparison of hovering performance of original main rotor blades with theory. Theory from NACA TN 626 (reference 1): $\sigma = 0.060$, constant chord; HNS-1 helicopter.

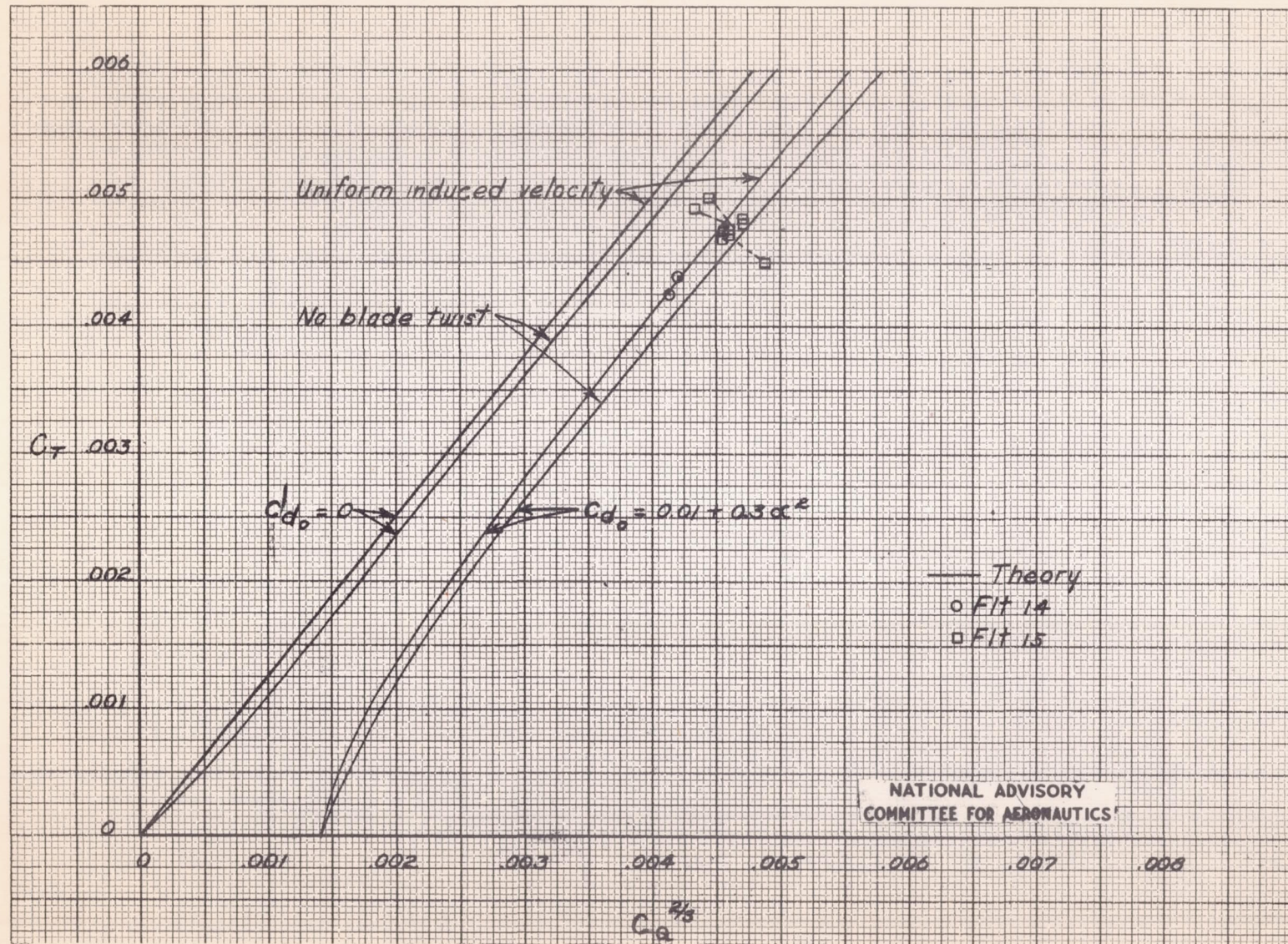


Figure 5.- Comparison of hovering performance of alternate main-rotor blades with theory. Theory from NACA 626 (reference 1): $\sigma = 0.042$, constant chord; HNS-1 helicopter.

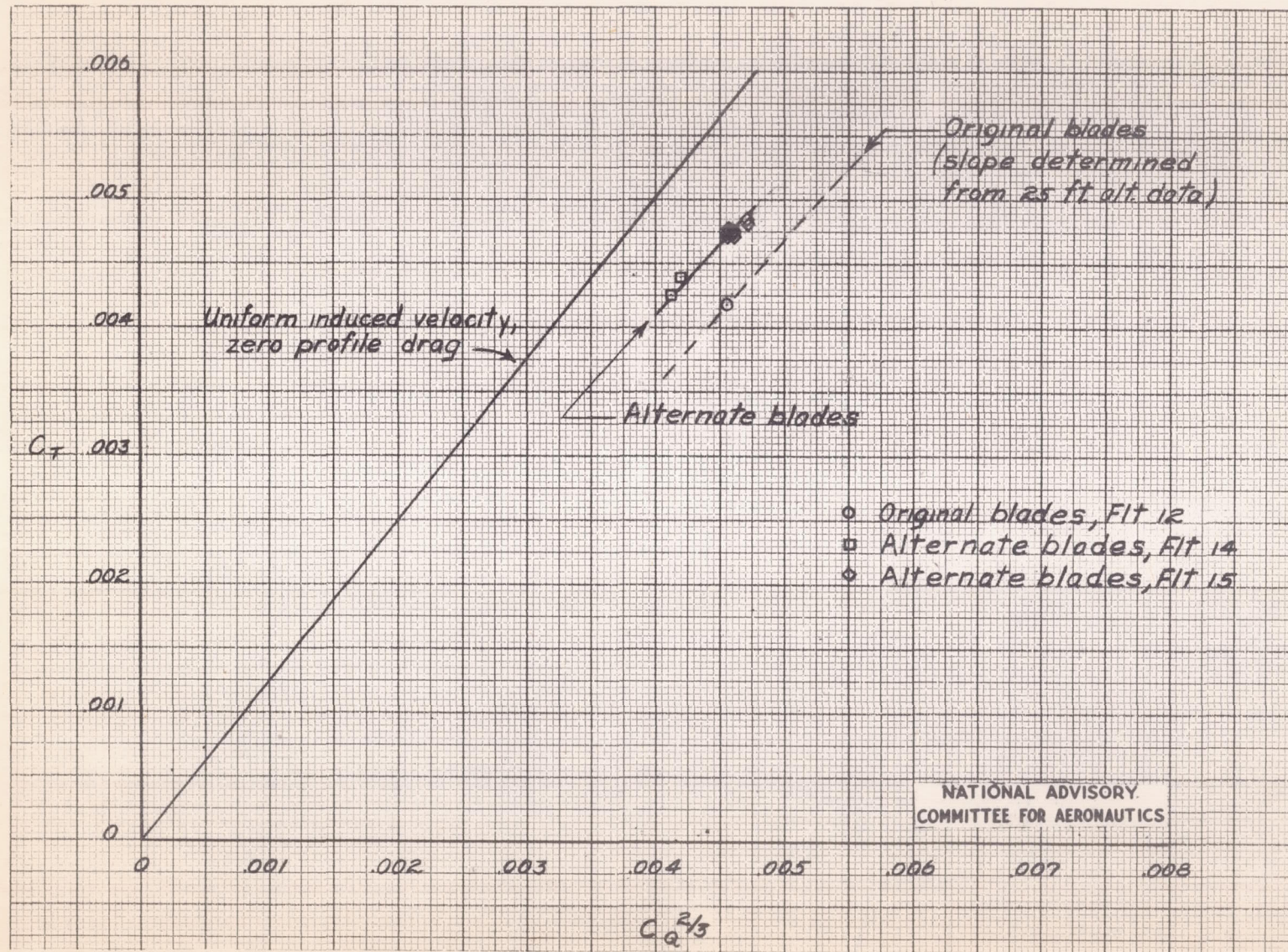


Figure 6.- Comparison of hovering performance of original main-rotor blades and alternate main-rotor blades; HNS-1 helicopter.

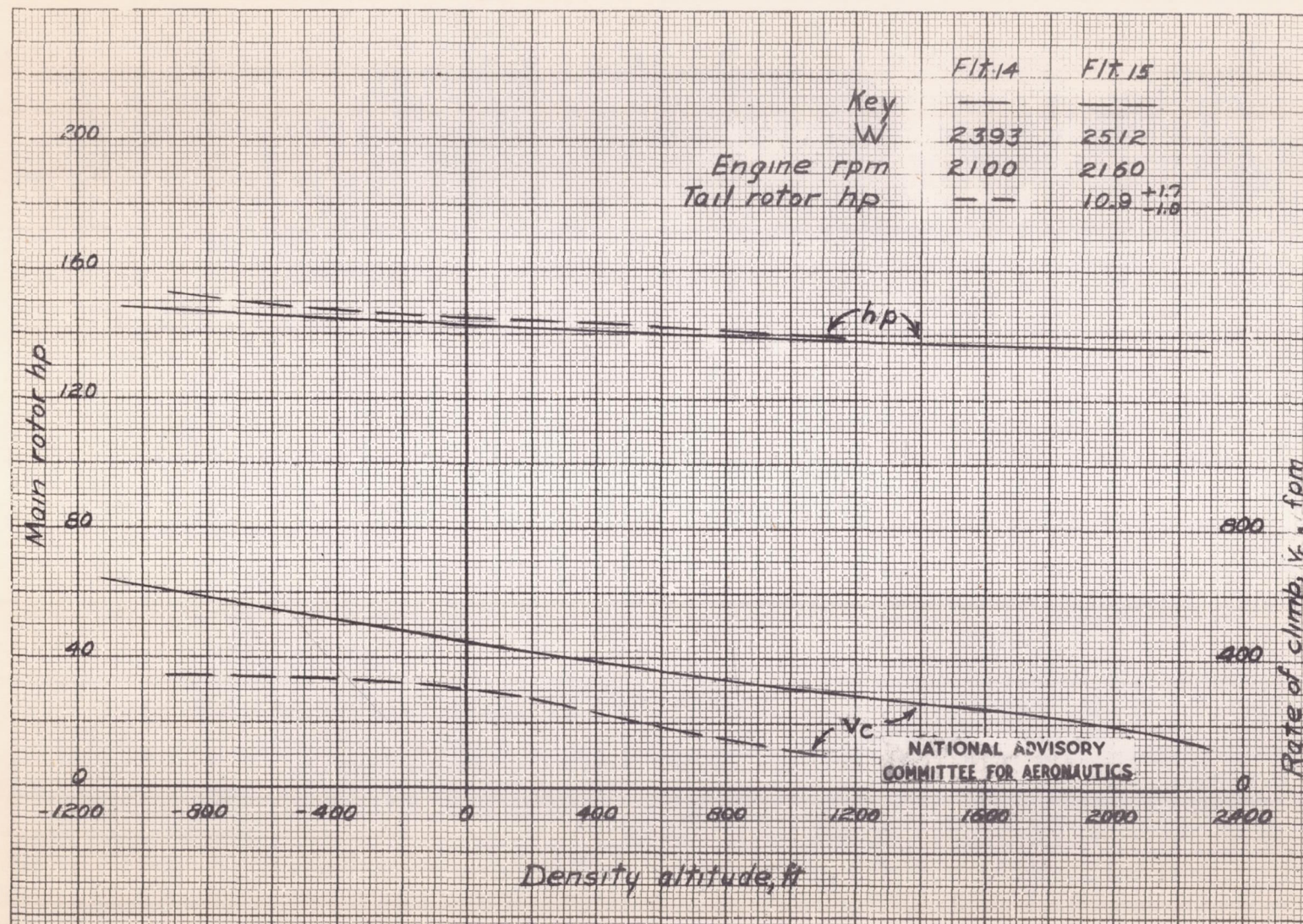


Figure 7.- Continuous climb records obtained with alternate main-rotor blades; HNS-1 helicopter.

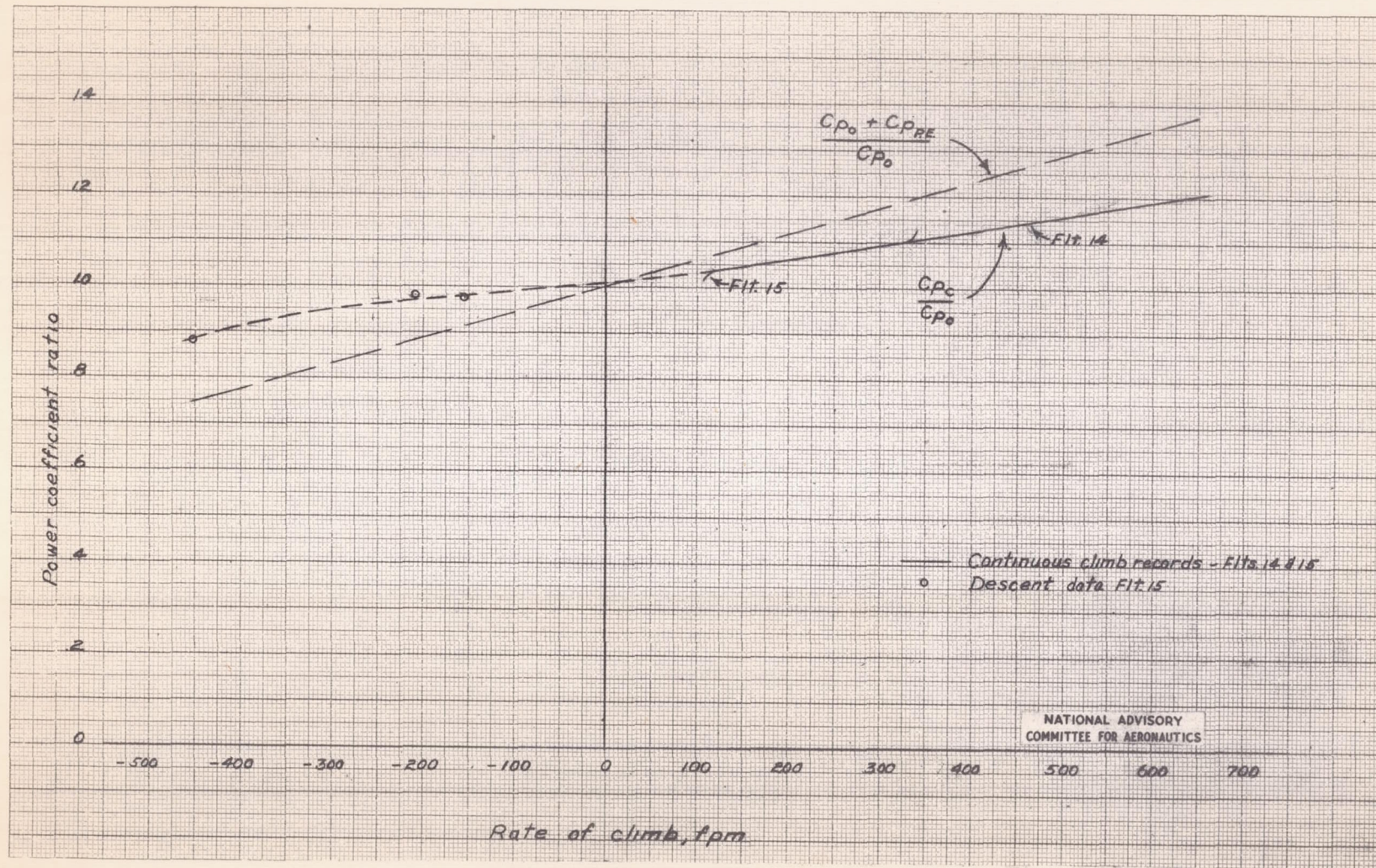


Figure 8.- Effect of rates of climb and descent on main rotor efficiency; HNS-1 helicopter.